

14

High-precision low-energy QED tests

As shown in the previous chapter, one expects that QED works well until an astronomical value of Λ_{em} , which is due to the non-asymptotically free property of the theory, where the effective charge grows with the energy. Therefore, contrary to QCD, one expects that QED is best tested at low energies which is the interesting experimental region.¹

14.1 The lepton anomaly

Indeed, one of the most impressive and traditional test of QED is given by the measurements of the leptons (e , μ) anomalous magnetic moments (lepton anomaly) a_μ , where one notices that from the electron to the muon, the running charge has increased from $\bar{\alpha}(t=0)$ to $\bar{\alpha}(t=\ln(m_\mu/m_e))$. The anomalous magnetic moment of charged leptons and for on-shell photon ($q^2=0$) is defined as:

$$a_l \equiv \frac{1}{2}(g_l - 2) \equiv F_2(0), \quad (14.1)$$

where $F_2(0)$ is the Pauli form factor related to the lepton-photon-lepton vertex as:

$$\bar{u}(p')\Gamma_\mu(p^2 = p'^2 = m^2)u(p) = \bar{u}(p')\gamma_\mu u(p)F_1(q^2) - \frac{1}{2m}\bar{u}(p')\sigma_{\mu\nu}q^\nu u(p)F_2(q^2). \quad (14.2)$$

The full vertex and the lowest order QED contribution are given by Fig. 14.1.

The lowest order contribution is:

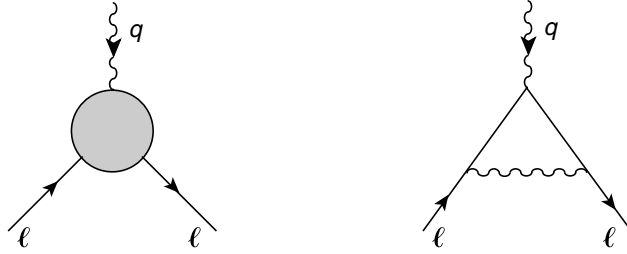
$$a_l^{(2)} = \frac{1}{2}\left(\frac{\alpha}{\pi}\right). \quad (14.3)$$

14.1.1 The electron anomaly and measurement of fine structure constant α

In the case of the electron, the anomalous magnetic moment has been measured with a high accuracy [181]:

$$\begin{aligned} a_{e^-}^{\text{exp}} &= 115\,965\,218\,84(43) \times 10^{-13}, \\ a_{e^+}^{\text{exp}} &= 115\,965\,218\,79(43) \times 10^{-13}. \end{aligned} \quad (14.4)$$

¹ For some other low-energy tests of the fermion substructure beyond the standard model, see e.g. [180].

Fig. 14.1. Full vertex and lowest order QED contribution to a_l .

A comparison of this value with the theoretical prediction [182,183,184]:

$$a_e^{\text{SM}} = \frac{1}{2} \left(\frac{\alpha}{\pi} \right) - 0.328\,478\,444\,00 \left(\frac{\alpha}{\pi} \right)^2 + 1.181\,234\,017 \left(\frac{\alpha}{\pi} \right)^3 \\ - 1.509\,8(384) \left(\frac{\alpha}{\pi} \right)^4 + 1.66(3) \times 10^{-12} (\text{hadronic} + \text{electroweak loops}) \quad (14.5)$$

provides a very precise measurement of the QED charge (fine structure constant) at the scale of the electron mass [185]:

$$\alpha^{-1}(a_e) = 137.035\,999\,58(52), \quad (14.6)$$

which is more precise than the one from the quantum Hall effect [182]:

$$\alpha^{-1}(\text{Hall}) = 137.036\,003\,00(270). \quad (14.7)$$

A resolution of the two discrepancies can provide a bound on new physics which is however not very strong as the new physics scale is constrained to be only larger than 100 GeV, assuming a generic effect of the order of m_e^2/Λ^2 .

14.1.2 The muon anomaly and the rôle of the hadronic contributions

In the case of the muon, higher order QED contributions are known up order α^5 . Typical higher order QED diagrams are shown in Fig. 14.2.

The total QED contribution reads [184,186]:

$$a_\mu^{\text{QED}} = \frac{1}{2} \left(\frac{\alpha}{\pi} \right) + 0.765\,857\,376(27) \left(\frac{\alpha}{\pi} \right)^2 + 24.050\,508\,98(44) \left(\frac{\alpha}{\pi} \right)^3 \\ + 126.07(41) \left(\frac{\alpha}{\pi} \right)^4 + 930(170) \left(\frac{\alpha}{\pi} \right)^5 \\ = 116\,584\,705.7(2.9) \times 10^{-11}. \quad (14.8)$$

The electroweak contributions are known. In the standard model, the lowest order contributions come from Fig. 14.3.

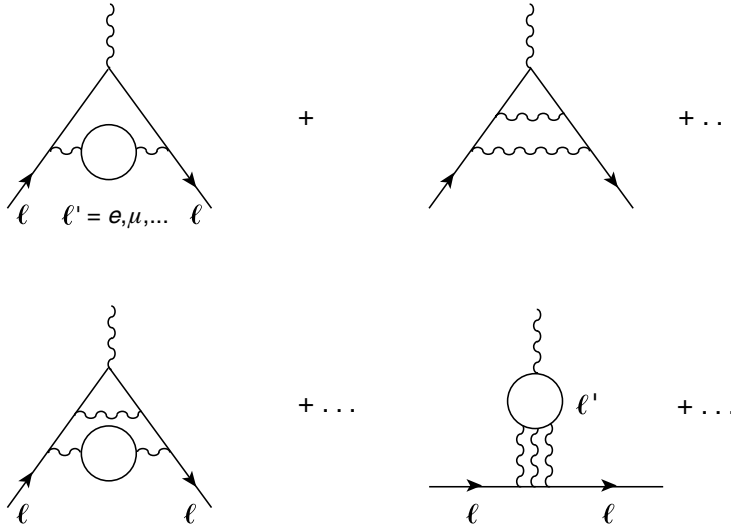


Fig. 14.2. Typical higher order QED contributions to a_l .

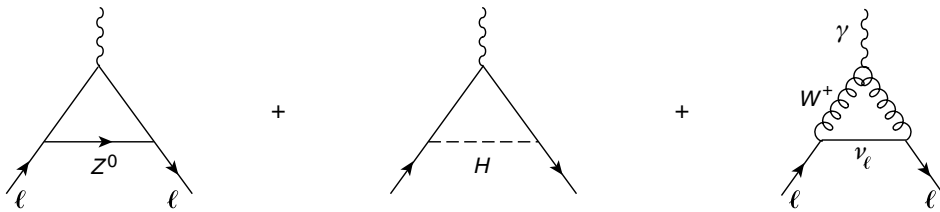


Fig. 14.3. Lowest order electroweak contribution to a_l .

It reads [186]:

$$a_\mu^{\text{EW}}(1 - \text{loop}) = \frac{G_\mu m_\mu^2}{8\sqrt{2}} \frac{5}{3\pi^2} \left[1 + \frac{1}{5}(1 - 4 \sin^2 \theta_W)^2 + \mathcal{O}\left(\frac{m_\mu}{M}\right)^2 \right] \simeq 195 \times 10^{-11}, \tag{14.9}$$

where the $G_\mu = 1.16637(1) \times 10^{-5} \text{ GeV}^2$, $\sin^2 \theta_W = 0.223$ and M denotes M_W or M_{Higgs} . The full two-loop contribution including hadronic electroweak loops and a leading log-resummation is [186]:

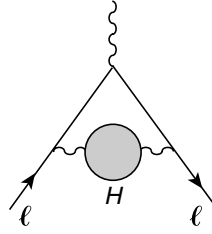
$$a_\mu^{\text{EW}}(2 - \text{loop}) = -43(4) \times 10^{-11} \tag{14.10}$$

and gives the total contribution:

$$a_\mu^{\text{EW}} = 152(4) \times 10^{-11}. \tag{14.11}$$

14.1.3 The lowest order hadronic contributions

The main theoretical errors in the determination of the muon anomalous magnetic moment are due to the strong interaction (hadronic loop) contributions, in the region

Fig. 14.4. Lowest order hadronic contributions to a_l .

below 2 GeV, and mainly in the ρ meson region. The lowest order diagram is depicted in Fig. 14.4.

Using a dispersion relation, the hadronic vacuum polarization contribution to the muon anomaly can be expressed as [187–191]:

$$a_\mu^{\text{had}}(l.o) = \frac{1}{4\pi^3} \int_{4m_\pi^2}^{\infty} dt K_\mu(t) \sigma_H(t). \quad (14.12)$$

$K_\mu(t)$ is the QED kernel function [192]:

$$\begin{aligned} K_\mu(t) &= \int_0^1 dx \frac{x^2(1-x)}{x^2 + (t/m_\mu^2)(1-x)} \\ &= z_\mu^2 \left(1 - \frac{z_\mu^2}{2}\right) + (1+z_\mu)^2 \left(1 + \frac{1}{z_\mu^2}\right) \\ &\quad \times \left[\ln(1+z_\mu) - z_\mu + \frac{z_\mu^2}{2} \right] \\ &\quad + \left(\frac{1+z_\mu}{1-z_\mu} \right) z_\mu^2 \ln z_\mu, \end{aligned} \quad (14.13)$$

with:

$$z_\mu = \frac{(1-v_\mu)}{(1+v_\mu)}, \quad \text{and} \quad v_\mu = \sqrt{1 - \frac{4m_\mu^2}{t}}. \quad (14.14)$$

$K_\mu(t)$ is a monotonically decreasing function of t . For large t , it behaves as:

$$K_\mu(t > m_\mu^2) \simeq \frac{m_\mu^2}{3t}, \quad (14.15)$$

which will be useful for the analysis in the large t regime. Such properties then emphasize the importance of the low-energy contribution to $a_\mu^{\text{had}}(l.o)$, where the QCD theory cannot be (strictly speaking) applied. $\sigma_H(t) \equiv \sigma(e^+e^- \rightarrow \text{hadrons})$ is the $e^+e^- \rightarrow \text{hadrons}$ total cross-section which can be related to the hadronic two-point spectral function $\text{Im}\Pi(t)_{\text{em}}$ through the optical theorem:

$$R_{e^+e^-} \equiv \frac{\sigma(e^+e^- \rightarrow \text{hadrons})}{\sigma(e^+e^- \rightarrow \mu^+\mu^-)} = 12\pi \text{Im}\Pi(t)_{\text{em}}, \quad (14.16)$$

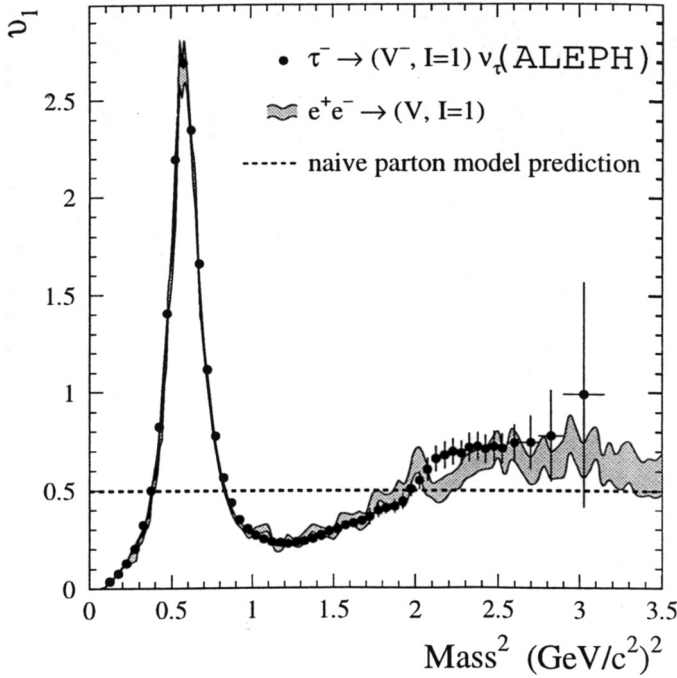


Fig. 14.5. Isovector spectral function from tau-decay and comparison with the e^+e^- data.

where:

$$\sigma(e^+e^- \rightarrow \mu^+\mu^-) = \frac{4\pi\alpha^2}{3t} . \tag{14.17}$$

Here,

$$\begin{aligned} \Pi_{em}^{\mu\nu} &\equiv i \int d^4x e^{iqx} \langle 0 | T J_{em}^\mu(x) (J_{em}^\nu(x))^\dagger | 0 \rangle \\ &= -(g^{\mu\nu}q^2 - q^\mu q^\nu) \Pi_{em}(q^2) \end{aligned} \tag{14.18}$$

is the correlator built from the local electromagnetic current:

$$J_{em}^\mu(x) = \frac{2}{3} \bar{u} \gamma^\mu u - \frac{1}{3} \bar{d} \gamma^\mu d - \frac{1}{3} \bar{s} \gamma^\mu s + \dots \tag{14.19}$$

The present most precise result comes from combining the $e^+e^- \rightarrow$ hadrons compiled in [193–198,16] and the precise τ -decay data [193,199]. These data are shown in Fig. 14.5.

An average of the results from $e^+e^- \rightarrow$ hadrons: $a_\mu^{\text{had}}[e^+e^-] = 7016(119) \times 10^{-11}$ and τ decay $a_\mu^{\text{had}}[\tau] = 7036(76) \times 10^{-11}$ data leads to [201]:

$$a_\mu^{\text{had}}(l.o) = 7021(76) \times 10^{-11} , \tag{14.20}$$

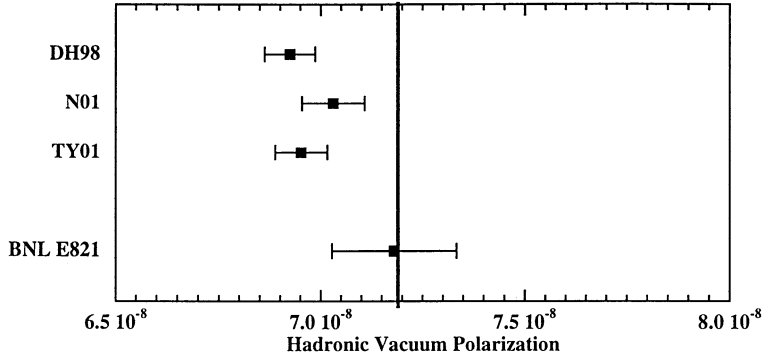


Fig. 14.6. Lowest order hadronic vacuum polarization contributions to a_μ from [207].

where the CVC hypothesis has been used in order to relate the electromagnetic to the charged current through an isospin rotation [200]:

$$\sigma_H(t) = \frac{4\pi\alpha^2}{t} v_1, \quad (14.21)$$

and where a correction due to the $\omega - \rho$ mixing has been applied. We follow the notation of ALEPH [193], where:

$$\text{Im}\Pi_{\bar{u}d,V}^{(1)} \equiv \frac{1}{2\pi} v_1, \quad (14.22)$$

is the charged vector two-point correlator:

$$\begin{aligned} \Pi_{\bar{u}d,V}^{\mu\nu} &\equiv i \int d^4x e^{iqx} \langle 0 | T J_{\bar{u}d}^\mu(x) (J_{\bar{u}d}^\nu(0))^\dagger | 0 \rangle \\ &= -(g^{\mu\nu} q^2 - q^\mu q^\nu) \Pi_{\bar{u}d,V}^{(1)}(q^2) \\ &\quad + q^\mu q^\nu \Pi_{\bar{u}d,V}^{(0)}(q^2), \end{aligned} \quad (14.23)$$

built from the local charged current $J_{\bar{u}d,V}^\mu(x) = \bar{u}\gamma^\mu d(x)$. It is amusing to notice that the central value here coincide with the old result in [209,215]. In [202], the impressive agreement of the result of the hadronic contributions to the QED running coupling α and to the muonium hyperfine splitting with other determinations (see next section) is a strong support of the estimate obtained in [201]. In Fig. 14.6, we see that the most recent standard model theoretical determinations [205,201] are in good agreement with the measured value [206,207]. After the completion of this work, we became aware of recent determinations [203] using recent $e^+e^- \rightarrow$ hadrons data from CMD-2 and BES [204] and of more precise measurement of $a_\mu^{\text{exp}} = 11\,659\,204(7) (5) \times 10^{-10}$ [208]. The estimate based on τ -decay agrees with ours whereas the one from e^+e^- differs by 1.4σ from ours, and leads to a discrepancy of 3σ between a_μ^{exp} and a_μ^{SM} of the Standard Model predictions. However, a new analysis of the scalar meson contributions (SN, hep-ph/0303004) gives an additional effect $a_\mu^S \leq 13(11) 10^{-10}$, which reduces the discrepancy of a_μ^{SM} and a_μ^{exp} . The difference between the results from e^+e^- and τ decay still needs to be understood.

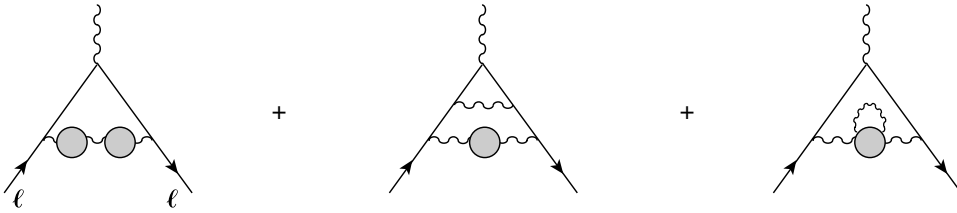


Fig. 14.7. Higher order hadronic vacuum polarization contributions to a_l .

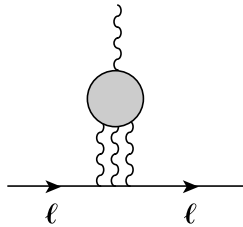


Fig. 14.8. Light-by-light scattering hadronic contribution to a_μ .

14.1.4 The higher order hadronic contributions

Higher order contributions were first discussed in [209]. They can be divided into two classes. The one involving the vacuum polarization is given in Fig. 14.7, and can be related to the measured $e^+e^- \rightarrow$ hadrons total cross-section, similar to the lowest order contribution. It gives [201] after rescaling the result in [209,210]:

$$a_\mu^{\text{had}}(h.o.)_{\text{VP}} = -101.2(6.1) \times 10^{-11} , \tag{14.24}$$

The second class is the light-by-light scattering diagram shown in Fig. 14.8.

Contrary to the case of vacuum polarization, this contribution is not yet related to a direct measurable quantity. In order to estimate this contribution, one has to introduce some theoretical models. The ones used at present are based on chiral perturbation [211] and ENJL model [212], where to both are added vector meson dominance and phenomenological parametrization of the pion form factors. The different contributions can be classified in diagrams Fig. 14.9, where the first two come from the quark (constituent) and boson loops, whereas the last one is due to meson pole exchanges. The first two diagrams are quite sensitive to the effects of rho-meson attached at the three off-shell photon legs which reduce the contributions by about one order of magnitude. The third diagram with pseudoscalar meson exchanges (anomaly) gives so far the most important contribution. There is a complete agreement between the two model estimates (after correcting the sign of the pseudoscalar and axial-vector contributions [213]), which may indirectly indicate that the results obtained are model independent. However, there are still some subtle issues left to be understood (is the inclusion of a quark loop a double counting?; why the inclusion of the rho-meson decreases drastically the quark and pion loop contributions?; is a single pole dominance

Table 14.1. $a_\mu^{\text{had}}(h.o)_{\text{LL}} \times 10^{11}$

Type of diagrams	[211]	[212]
π^- loop	-4.5(8.1)	-19(13)
quark loop (not added in the sum)	9.7(11)	21(3)
π^0, η, η' poles	82.7(6.4)	85(13)
axial-vector pole	1.74	2.5(1.0)
scalar pole		-6.8(2.0)
Total	79.9(18.2)	61.7(23.8)

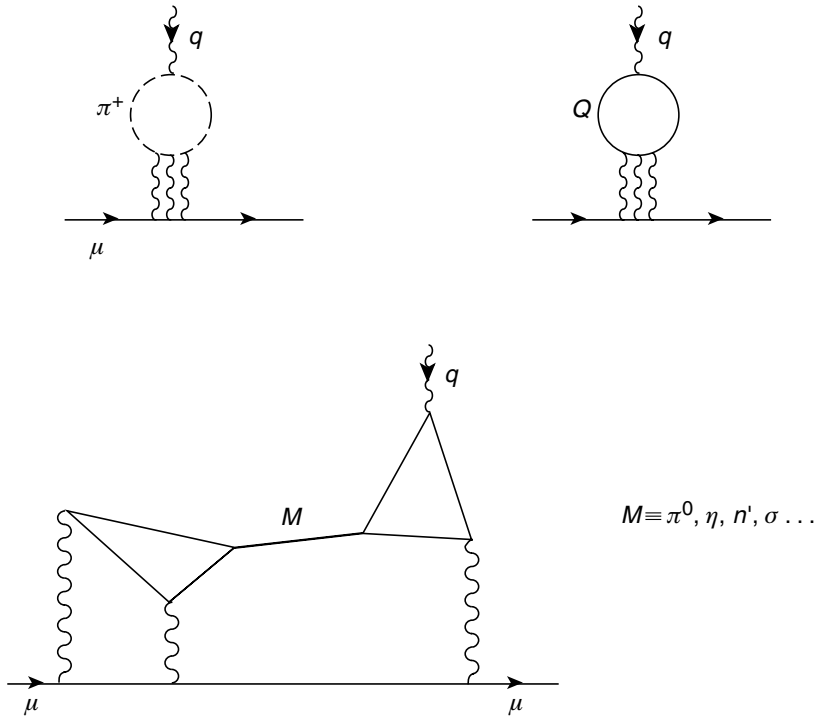


Fig. 14.9. Different light-by-light scattering hadronic contributions to a_μ .

justified?, . . .). The results in [211] and [212], after correcting the sign of the pseudoscalar and axial-vector contributions [213], are given in Table 14.1.

An arithmetic average of the central values and of the errors give:

$$a_\mu^{\text{had}}(h.o)_{\text{LL}} = 70.8(21.0) \times 10^{-11} . \tag{14.25}$$

One can remark the agreement in sign and magnitude with the contribution of a quark constituent loop diagram (first used in [209]) without any hadrons [214] and YT01 in [205].

Then, we deduce:

$$a_\mu^{\text{had}}(h.o) = a_\mu^{\text{had}}(h.o)_{\text{VP}} + a_\mu^{\text{had}}(h.o)_{\text{LL}} = -30.4(21.9) \times 10^{-11}, \quad (14.26)$$

where one can notice a partial cancellation between the higher order vacuum polarization and the light-by-light scattering contributions.

14.1.5 The total theoretical contributions to a_μ

Summing up different contributions, the present theoretical status in the standard model is:

$$\begin{aligned} a_\mu^{\text{SM}} &= a_\mu^{\text{QED}} + a_\mu^{\text{EW}} + a_\mu^{\text{had}} \\ &= 116\,584\,669.9(39.2) \times 10^{-11} + a_\mu^{\text{had}}(l.o.) \\ &= 116\,591\,846.9(78.9) \times 10^{-11}. \end{aligned} \quad (14.27)$$

This theoretical contribution can be compared with the experimental average [186] of CERN78 [216] + BNL98 [207] + BNL99 [208]:

$$a_\mu^{\text{exp}}(\text{average}) = 116\,592\,023(151) \times 10^{-11}. \quad (14.28)$$

which is more weighted by the new BNL precise result:

$$a_\mu^{\text{exp}}(\text{BNL99}) = 116\,592\,020(160) \times 10^{-11}. \quad (14.29)$$

The comparison of the theoretical and experimental numbers gives:

$$a_\mu^{\text{new}} \equiv a_\mu^{\text{exp}} - a_\mu^{\text{SM}} = (176 \pm 170) \times 10^{-11}, \quad (14.30)$$

which can indicate about σ deviation from the SM prediction. This result can be used to give a lower bound on the presence of new physics beyond the standard model. Combining this result with the world average of $a_\mu^{\text{had}}(l.o.)$, we can have the range at 90% confidence level (CL):

$$-42 \leq a_\mu^{\text{new}} \times 10^{11} \leq 413 \quad (90\% \text{ CL}). \quad (14.31)$$

This range is expected to be improved in the near future both from accurate measurements of a_μ and of e^+e^- data necessary for reducing the theoretical errors in the determinations of the hadronic contributions, being the major source of the theoretical uncertainties. Constraints on some models (supersymmetry, radiative muon mass, leptoquarks) beyond the standard model (SM) using this result have been discussed in [186,201]. The lower bounds on the scale of the models using this new allowed range of a_μ^{new} are typically:

$$\begin{aligned} \tilde{m} &\geq 113 \text{ GeV} && : \text{ degenerate sparticle mass} \\ M &\geq 1.7 \text{ TeV} && : \text{ compositeness} \\ M_{S_2} &\geq 55.5 \text{ GeV} && : \text{ Zee model singlet scalar} \\ M &\geq 1.1 \text{ TeV} && : \text{ leptoquarks.} \end{aligned} \quad (14.32)$$

14.1.6 The τ anomaly

The different theoretical contributions to the τ anomaly have been discussed before in [215]. Compared to the case of the electron and of the muon, an eventual precise measurement of a_τ will provide a further test of the QED calculation at short distance $t = \ln(M_\tau/m_l)$ not reached in the electron and muon case. Then, it can provide a measurement of the QED running coupling $\bar{\alpha}$ as given by the RGE discussed previously, and a test of an eventual sub-structure of the τ lepton. As can be seen in details in [215], the relative weight of the hadronic contributions has decreased compared, for example, with the weak interaction contributions. Also, because of the large value of M_τ , the rôle of the ρ -meson has relatively decreased, which renders, almost equal, the contribution of the hadrons below and above 1 GeV. This is a positive feature which can allow a precise theoretical prediction of this observable. An update of the theoretical predictions obtained in [215] is [201] (in units of 10^{-8}):

$$\begin{aligned} a_\tau^{\text{QED}} &= 117\,327.1(1.2), \\ a_\tau^{\text{EW}} &\simeq 46.9(1.2), \\ a_\tau^{\text{had}}(l.o) &= 353.6(4.0), \\ a_\tau^{\text{had}}(h.o)_{\text{(LL)}} &= 20.0(5.8), \\ a_\tau^{\text{had}}(h.o) &= 27.6(5.8), \end{aligned} \tag{14.33}$$

which leads to:

$$\begin{aligned} a_\tau^{\text{SM}} &= a_\tau^{\text{had}} + a_\tau^{\text{EW}} + a_\tau^{\text{QED}} \\ &= 117\,755.2(7.2) \times 10^{-8}. \end{aligned} \tag{14.34}$$

where we have used the present accurate value of $M_\tau = 1.77703$ GeV. This value in Eq. (14.34) can be compared with the present (inaccurate) experimental value [217]:

$$a_\tau^{\text{exp}} = 0.004 \pm 0.027 \pm 0.023, \tag{14.35}$$

which, we hope, can be improved in the near future.

14.2 Other high-precision low-energy tests of QED

14.2.1 Lowest order hadronic contributions

In addition to the high-precision measurements of the lepton anomalies, some QED high-precision tests are also performed. As in the case of the lepton anomalies, the hadronic contributions also play an important for the QED predictions of the running QED coupling $\alpha(M_Z)$ and of the muonium hyperfine splittings ν . These contributions can be expressed in a closed form as the convolution integral:²

$$\mathcal{O}_{\text{had}} = \frac{1}{4\pi^3} \int_{4m_\pi^2}^{\infty} dt K_{\mathcal{O}}(t) \sigma_H(t), \tag{14.36}$$

² For a recent estimate and review see e.g. Ref. [202] and references therein.

where:

$$\mathcal{O}_{\text{had}} \equiv \Delta\alpha_{\text{had}} \times 10^5 \quad \text{or} \quad \Delta\nu_{\text{had}} . \tag{14.37}$$

- For the QED running coupling $\Delta\alpha_{\text{had}} \times 10^5$, the kernel is:

$$K_\alpha(t) = \left(\frac{\pi}{\alpha}\right) \left(\frac{M_Z^2}{M_Z^2 - t}\right) , \tag{14.38}$$

where $\alpha^{-1}(0) = 137.036$ and $M_Z = 91.3$ GeV. It behaves for large t like a constant.

- For the muonium hyperfine splitting $\Delta\nu_{\text{had}}$, the kernel function is (see e.g. [220]):

$$K_\nu = -\rho_\nu \left[(x_\mu + 2) \ln \frac{1 + v_\mu}{1 - v_\mu} - \left(x_\mu + \frac{3}{2}\right) \ln x_\mu \right] \tag{14.39}$$

where:

$$\rho_\nu = 2v_F \frac{m_e}{m_u} , \quad x_\mu = \frac{t}{4m_\mu^2} \quad v_\mu = \sqrt{1 - \frac{1}{x_\mu}} , \tag{14.40}$$

and v_F is the Fermi energy splitting:

$$v_F = 445\,903\,192\,0.(511)(34) \text{ Hz} . \tag{14.41}$$

It behaves for large t as:

$$K_\nu(t \gg m_\mu^2) \simeq \rho_\nu \left(\frac{m_\mu^2}{t}\right) \left(\frac{9}{2} \ln \frac{t}{m_\mu^2} + \frac{15}{4}\right) . \tag{14.42}$$

The different asymptotic behaviours of these kernel functions will influence on the relative weights of different regions contributions in the evaluation of the above integrals.

14.2.2 QED running coupling $\alpha(M_Z)$

Using the same data as for the anomalous magnetic moment, one can deduce the lowest order hadronic contribution [202]:

$$\Delta\alpha_{\text{had}} = 2763.4(16.5) \times 10^{-5} . \tag{14.43}$$

We add the hadronic radiative corrections $\Delta\alpha_{\text{had}} = (6.4 \pm 2.7) \times 10^{-5}$ from the radiative modes $\pi^0\gamma, \eta\gamma, \pi^+\pi^-\gamma \dots$ coming from the largest range given in [195] and YT01 [205]. Using the renormalization group evolution of the QED coupling:

$$\alpha^{-1}(M_Z) = \alpha^{-1}(0)[1 - \Delta\alpha_{\text{QED}} - \Delta\alpha_{\text{had}}] , \tag{14.44}$$

and the available results to three-loops [218] of $\Delta\alpha_{\text{QED}} = 3149.7687 \times 10^{-5}$, one can deduce:

$$\alpha^{-1}(M_Z) = 128.926(25) . \tag{14.45}$$

The results in Eqs. (14.43) and (14.45) are in good agreement with other determinations [205,219] as shown in Fig. 14.10, but more accurate, thanks to the combined e^+e^- and τ -decay data.

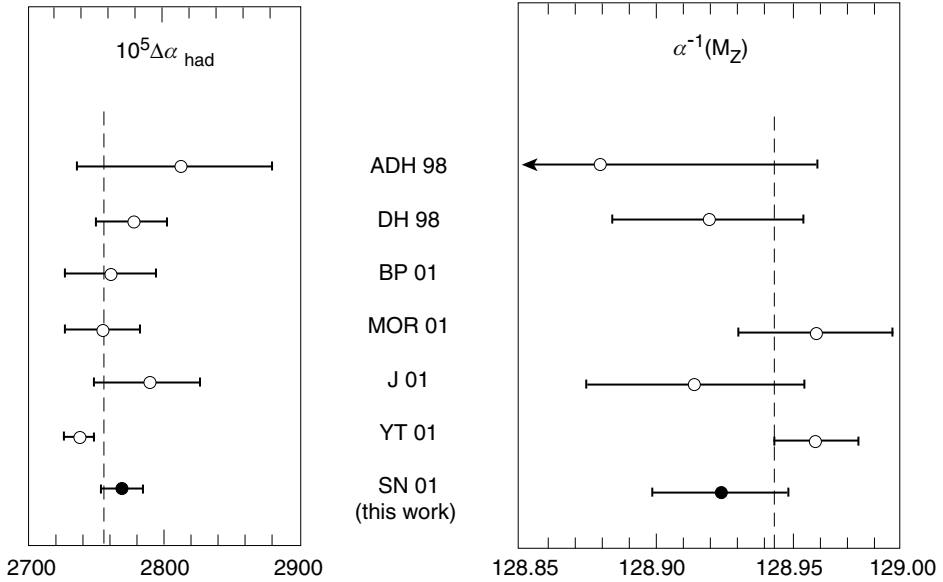


Fig. 14.10. Recent determinations of $\Delta\alpha_{\text{had}}$ and $\alpha^{-1}(M_Z)$. The dashed vertical line is the mean central value. References to the authors are in [218,219,195,205].

The above results are important for a precise determination of the Higgs mass from a global fit of the electroweak data as shown in Fig. 14.11.

We expect that with this new improved estimate, the present lower bound of 114 GeV for the Higgs mass from LEP data can be improved in the near future.

14.2.3 Muonium hyperfine splitting

Using again the same data input as in previous observables, the hadronic contribution to the muonium hyperfine splitting is [202]:

$$\Delta\nu_{\text{had}} = (232.5 \pm 3.2) \text{ Hz} , \tag{14.46}$$

which is in excellent agreement with recent determinations shown in Table 14.2.

Here, due to the $(\ln t)/t$ behaviour of the kernel function, the contribution of the low-energy region is dominant. However, the ρ -meson region contribution below 1 GeV is 47% compared with the 68% in the case of a_μ , while the QCD continuum is about 10% compared to 7.4% for a_μ . The accuracy of our result is mainly due to the use of the τ -decay data, explaining the similar accuracy of our final result with the one in [220] using new Novosibirsk data. Combined with existing QED and electroweak contributions:

$$\begin{aligned} \Delta\nu_{\text{QED}} &= 4\,270\,819(220) \text{ Hz} , & \Delta\nu_{\text{weak}}(l.o) &= -\frac{G_F}{\sqrt{2}} m_e m_\mu \left(\frac{3}{4\pi\alpha} \right) v_F \simeq -65 \text{ Hz} , \\ |\Delta\nu_{\text{weak}}(h.o)| &\approx 0.7 \text{ Hz} , & \Delta\nu_{\text{had}}(h.o) &\simeq 7(2) \text{ Hz} , \end{aligned} \tag{14.47}$$

Table 14.2. Recent determinations of Δv_{had}

Authors	Δv_{had} [Hz]
FKM 99 [221]	240 ± 7
CEK 01 [220]	233 ± 3
SN 01 [202]	232.5 ± 3.2

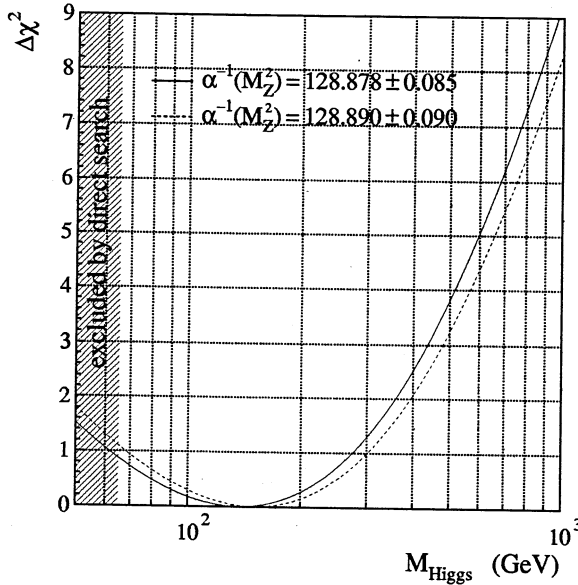


Fig. 14.11. χ^2 of the global fit determinations of the Higgs mass using electroweak data.

one obtains the SM prediction:

$$v_{\text{SM}} \equiv v_F + \Delta v_{\text{QED}} + \Delta v_{\text{weak}} + \Delta v_{\text{had}} + \Delta v_{\text{had}}(h.o), \tag{14.48}$$

from which one can, for example, deduce [202]:

$$\frac{v_{\text{SM}}}{v_F} = 1.000\,957\,83(5), \tag{14.49}$$

by noting that v_F enters as an overall factor in the theoretical contributions. Combining this result with the experimental value of v :

$$v_{\text{exp}} = 4\,463\,302\,776(51)\text{ Hz}, \tag{14.50}$$

one can deduce the SM prediction:

$$v_F^{\text{SM}} = 4\,459\,031\,783(226)\text{ Hz}, \tag{14.51}$$

where the error is dominated here by the QED contribution at fourth order. This result is a factor of 2 more precise than the one in [220]. One can use this result in Eq. (14.51) in the expression:

$$v_F = \rho_F \left(\frac{m_e}{m_\mu} \right) \frac{1}{(1 + m_e/m_\mu)^3} (1 + a_\mu) , \quad (14.52)$$

where $a_\mu = 1.165\,920\,3(15) \times 10^{-3}$, and:

$$\rho_F = \frac{16}{3} (Z\alpha)^2 Z^2 cR_\infty , \quad (14.53)$$

and $Z = 1$ for muonium, $\alpha^{-1}(0) = 137.035\,999\,58(52)$ [182,184], $cR_\infty = 3\,289\,841\,960\,368(25)$ kHz. Therefore, one can extract a value of the ratio of the muon over the electron mass:

$$\frac{m_\mu}{m_e} = 206.768\,276(11) , \quad (14.54)$$

to be compared with the PDG value 206.768 266(13) using the masses in MeV units. If one uses the relation:

$$v_F = \rho_F \left(\frac{\mu_\mu}{\mu_B^e} \right) \frac{1}{(1 + m_e/m_\mu)^3} , \quad (14.55)$$

one can also extract the one can deduce the ratio of magnetic moments:

$$\frac{\mu_\mu}{\mu_B^e} = 4.841\,970\,47(25) \times 10^{-3} , \quad (14.56)$$

compared with the one obtained from the PDG values of μ_μ/μ_p and μ_p/μ_B^e : $\mu_\mu/\mu_B^e = 4.841\,970\,87(14) \times 10^{-3}$. In both applications, the results in Eqs. (14.54) and (14.56) are in excellent agreement with the PDG values.

14.3 Conclusions

We have discussed the evaluation of the hadronic and QCD contributions $a_l^{\text{had}}(l.o)$, $\Delta\alpha_{\text{had}}$ and Δv_{had} respectively to the anomalous magnetic moment, the QED running coupling and to the Muonium hyperfine splitting. Our self-contained results derived from the same input data and QCD parameters are in excellent agreement with existing determinations and are quite accurate. One of the immediate consequences of these results is the prediction of a_μ , a_τ and $\alpha(M_Z)$. We have used the result for the muonium hyperfine splitting for a high precision measurement of the ratios of the muon over the electron mass and of their magnetic moments. These standard model predictions are in excellent agreement with those quoted by PDG [16] and can be used for providing strong constraints on some model building beyond the standard model.